AN OPEN-SOURCE-BASED WORKFLOW FOR DEM GENERATION FROM SENTINEL-1 FOR LANDSLIDE VOLUME ESTIMATION

L. Abad[1, *], D. Hölbling[1], Z. Dabiri[1], B. A. Robson[2]

[1] Department of Geoinformatics, University of Salzburg, 5020 Salzburg, Austria –
(lorena.abad, daniel.hoelbling, zahra.dabiri)@plus.ac.at
[2] Department of Earth Science, University of Bergen, 5020 Bergen, Norway - benjamin.robson@uib.no

Commission IV, WG IV/4

KEY WORDS: DEM generation, InSAR, Sentinel-1, landslide, volume estimation, open-source

ABSTRACT:

Digital elevation models (DEMs) serve as a basis for various geomorphological applications, such as, landform mapping, natural hazard assessment, and landslide characterisation. The inter-comparison of DEMs can be used to provide estimates of topographic change, for example, volume changes. Sentinel-1 synthetic aperture radar (SAR) data can be used to generate multitemporal topographic datasets using interferometric SAR (InSAR). Such analyses are often conducted using commercial software; however, a well-structured workflow based on free and open-source software (FOSS) increases the applicability and transferability of the DEM generation method and can facilitate the use of multi-temporal topographic analysis within the Earth Sciences. In this study, we aim to develop an open-source-based workflow for the generation of multi-temporal DEMs from Sentinel-1 data, and to explore their potential for landslide volume estimation using FOSS. We implemented this semi-automated and transferable workflow bundled in the open-source Python package "SliDEM", which relies on SNAP, SNAPHU, and several other open-source software for geospatial and geomorphological applications, all distributed within a Docker image. Two major landslides in Austria and Norway were selected to test, evaluate, and validate the workflow in terms of reliability, performance, reproducibility, and transferability. Even if the quality of the Sentinel-1-based DEMs varies among the study areas, the preliminary results are promising. However, there is a need for improvement and thorough analysis of the causes of elevation errors. A comprehensive evaluation of the influence of the perpendicular and temporal baselines, topography, land use/land cover, and other environmental conditions can be systematically assessed within the "SliDEM" workflow.

1. INTRODUCTION

Digital elevation models (DEMs) serve as a basis for various geomorphological applications, for example, landform mapping, erosion and natural hazard assessment, landslide characterisation, and as input for process modelling, among others. Access to timely, accurate and comprehensive information is crucial for such applications. Moreover, topographic data are a relevant source of information that can be used to assess and manage potential cascading hazards and risks such as landslide dam outburst floods or debris flows.

The intercomparison of topographic products, also known as DEM differencing, can be used to derive surface elevation and volumetric changes. Information on landslide volumes helps to understand the role of triggering events and landslides on landscape evolution (Bernard et al., 2021; Paulin et al., 2022), such as the river damming potential of landslides (Argentin et al., 2021). DEMs derived from different remote sensing data have been used to estimate landslide volumes. These include, for example, historical aerial photographs (Robson et al., 2022; Santangelo et al., 2022), Uncrewed Aerial Vehicle (UAV) imagery (Chang et al., 2020; Turner et al., 2015), optical high-resolution stereo satellite imagery (Atefi and Miura, 2021; Tsutsui et al., 2007), or Light Detection And Ranging (LiDAR) data (Bernard et al., 2021; Paulin et al., 2022; Ventura et al., 2011). However, the applicability of existing DEMs is often limited. While commercial imagery allows timely and high-resolution topographic products, the prohibitively high cost of acquisitions makes it challenging to compile multi-temporal stacks of DEMs. Freely available DEMs, on the other hand, typically have one defined timestamp (e.g., SRTM, Copernicus DEM) or present more stochastic errors.

Synthetic aperture radar (SAR) imaging has proven to be useful for measuring the surface topography using interferometric SAR (InSAR) techniques (Crosetto, 2002). InSAR measures radiation travel path variations as a function of the satellite position and time of acquisition, which allows the extraction of three-dimensional information using the phase difference (Bamler and Hartl, 1998). InSAR techniques are based on the processing of at least two complex SAR images covering the same area and acquired from slightly different viewpoints. Although SAR data offer promising opportunities for DEM generation, major challenges include: 1) the geometry of SAR observations and the limited applicability in mountainous terrain and steep hills, resulting in shadowing, foreshortening, or layover effects; 2) wavelength constraints, for example, the C-band interferometry is limited for dense vegetation compared to the L-band wavelength, which better penetrates vegetation; 3) decorrelation for certain land cover types; 4) constrains due to atmospheric changes between the times of two SAR image acquisitions, which may cause atmospheric disturbance on interferograms (Bürgmann et al., 2000). Despite these limitations, using SAR data and SAR interferometry techniques to generate DEMs can support systematic topographic monitoring.

Sentinel-1 SAR data (C-band) from the European Union's Earth observation (EO) programme Copernicus provide the opportunity to use free SAR data to generate multitemporal topographic datasets every 6 to 12 days. Sentinel-1 A & B data allow us to tackle some of the issues related to data costs and spatio-temporal availability. Moreover, the European Space Agency (ESA) guarantees the continuity of the Sentinel-1 mission with the planned launch of two further satellites, i.e., Sentinel-1 C & D. Sentinel-1

*Corresponding author

https://doi.org/10.5194/isprs-archives-XLVIII-4-W1-2022-5-2022

SAR data have often been used to detect surface deformation; however, few studies have addressed DEM generation (Braun, 2021). For example, Dabiri et al. (2020) tested Sentinel-1 for landslide volume estimation but highlighted the need for further research and systematic assessment of the accuracy of the generated DEMs.

InSAR analysis for DEM generation is often conducted using commercial software; however, a well-structured workflow based on free and open-source software (FOSS) increases the applicability and transferability of the DEM generation method. Although a general workflow for DEM generation from Sentinel-1 imagery based on InSAR has been described and documented (Alaska Satellite Facility DAAC, 2019; Braun, 2021, 2020), there is a need to streamline, harmonise and automate the required steps using open-source tools.

In this study, we aim to develop an open-source-based workflow for the generation of multi-temporal DEMs from Sentinel-1 data and to explore their potential for landslide volume estimation using FOSS. Two major landslides in Austria and Norway were selected to test, evaluate, and validate the workflow in terms of reliability, performance, reproducibility, and transferability.

2. WORKFLOW FOR DEM GENERATION AND VOLUME ESTIMATION

The proposed workflow generates pre- and post-event DEMs using Sentinel-1 SAR data for a defined area affected by a landslide event and estimates the landslide volume computed from the DEM of Differences (DoD), as shown in Figure 1.

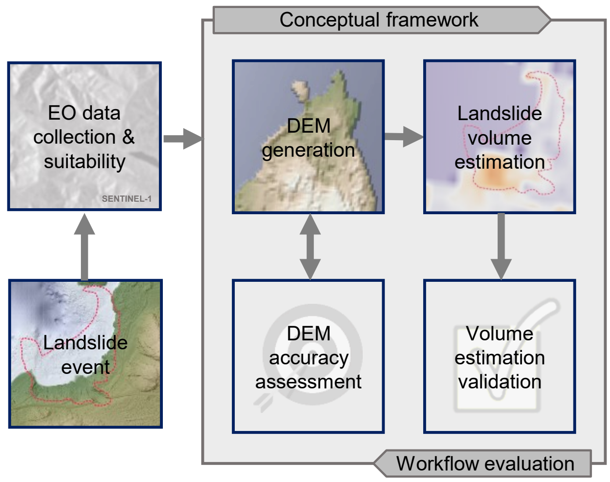

Figure 1: Conceptual workflow for DEM generation and landslide volume estimation

Once the area of interest (AOI) is defined, the first step is to find suitable Sentinel-1 image pairs that cover the study area and a designated time interval. Moreover, desired perpendicular and temporal baselines must be defined. The pre-selected image pairs are downloaded and used for DEM generation.

The steps to generate DEMs using InSAR techniques have been documented and described by Braun (2021), where the main steps include: 1) co-registration and debursting of Sentinel-1 image pairs, 2) interferogram generation, phase filtering, and multilooking, 3) phase unwrapping, and 4) conversion to elevation values and geometric correction. These steps are performed through the open-source Sentinel Application Platform (SNAP) developed by the ESA (European Space Agency, 2022) in combination with the Statistical-Cost, Network-Flow Algorithm for Phase Unwrapping (SNAPHU) developed by Stanford University (Chen and Zebker, 2002), through either a graphical user interface (GUI), a command line interface (CLI), or Python application programming interfaces (APIs) that wrap the Java implementation of SNAP.

The generated DEMs must be vertically aligned before computing the DoD and, consequently, estimating the landslide volume. The DEMs and estimated volumes are then compared to reference data to assess their quality and validate the results using statistical error measurements. The quality assessment evaluates the results based on the land use/land cover (LULC), the topography of the terrain, and the use of ascending and descending passes, among other factors, to identify the accuracy of the generated DEMs in different settings.

We implemented this semi-automated and transferable workflow bundled in an open-source Python package “SliDEM”, which relies on APIs connecting to SNAP, SNAPHU, and several other open-source software publicly available for geospatial and geomorphological applications. We distribute the “SliDEM” package within a Docker image, which allows its usage along with all its software dependencies in a structured and straightforward way, reducing usability problems related to software versioning and different operating systems.

3. TECHNICAL IMPLEMENTATION OF CONCEPTUAL WORKFLOW

The Python implementation of the workflow within the “SliDEM” package consists of five modules to 1) query Sentinel-1 image pairs; 2) download and archive suitable Sentinel-1 image pairs; 3) produce DEMs using InSAR techniques; 4) perform necessary post-processing such as terrain correction and co-registration and assess the quality and accuracy of the generated DEMs; and 5) perform DEM differencing of pre- and post-event DEMs to quantify landslide volumes and validate the volume estimates against reference data (Figure 2).

The *query* module fetches information from the Alaska Satellite Facility (ASF) using the Python wrapper for the ASF Search API (Alaska Satellite Facility Discovery Team, 2022). Initially, a geographical search is performed based on the given AOI and time interval. Next, we loop over the matching scenes to obtain paired scenes that fall between the perpendicular (B_{perp}) and temporal (B_{temp}) baseline thresholds using the baseline search. The image pairs correspond to the same relative pass (ascending or descending) and path. The result is a CSV file that includes only those Sentinel-1 scenes that match the geographic and temporal extents and the baseline (B_{perp} and B_{temp}) thresholds.

The analyst is directed to check the listed image pairs. A link to an optical Sentinel-2 image from the same time period within the Sentinel Hub Explorer tool is provided. This supports the visual assessment of current conditions on site to avoid downloading scenes that might result in problems during DEM generation due to, for example, snow cover. The analyst can then decide which image pairs to download within the CSV file. Once this is done, the CSV file and a download directory are passed to the *download* module; the scenes are downloaded from the ASF server.

Once Sentinel-1 scenes are downloaded and archived, the image pairs can be passed onto the *dem* module. The input parameters include an output directory, where the results are saved, and the AOI as a bounding box, which serves to subset the Sentinel-1 scene and therefore allows faster computation. Moreover, several

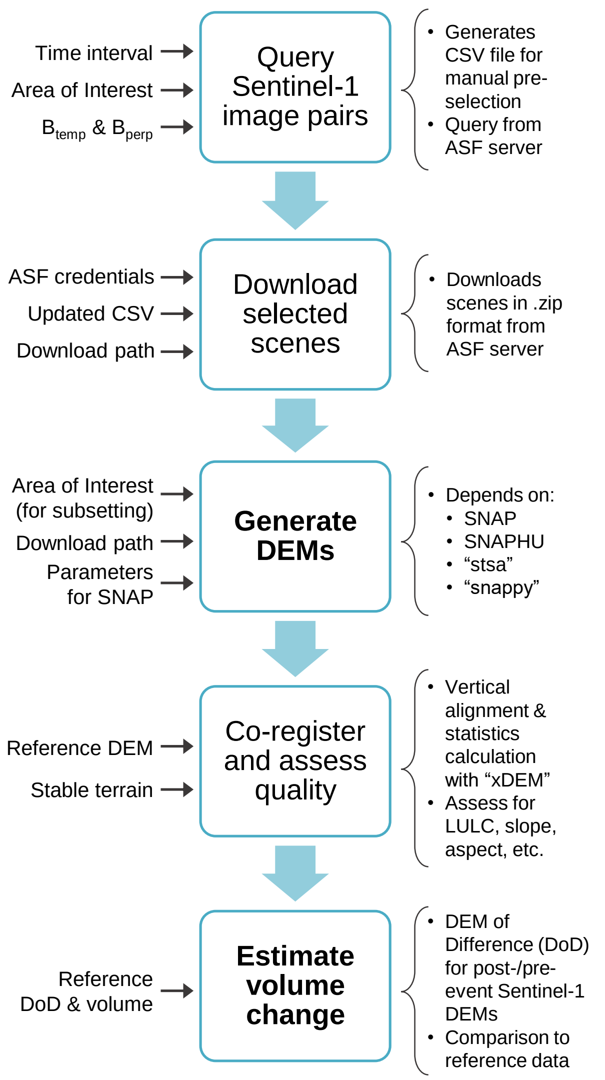

Figure 2: Modules of "SliDEM" Python package. B_{temp}: temporal baseline, B_{perp}: perpendicular baseline

parameters are passed onto the SNAP and SNAPHU functions such as the desired polarisation, DEM for back geo-coding, number of range-looks for multi-looking, number of tiles, and cost mode for SNAPHU export, among others (c.f. Braun 2021).

To connect to SNAP, we use the *snappy* Python package (European Space Agency and Brockmann Consult, 2022), while a migration to *snapista* (Brito, 2022) is envisioned as recommended by the ESA due to the stability and active development of the latter. To perform phase unwrapping, we used the CLI implementation of SNAPHU. As part of the automation process for DEM generation, we include an automatic extraction of sub-swaths and bursts that intersect the AOI, using the *stsa* (S-1 TOPS SPLIT Analyzer) Python package (Brotoisworo, 2021).

The *quality* module performs vertical alignment and assesses the quality and accuracy of the DEM generated from Sentinel-1 when compared to a reference DEM. For this, we use the *xDEM* Python package (Dehecq et al., 2021), which supports different horizontal and vertical alignment techniques. For example, the method set out by Nuth and Kääb (2011) assesses normalised elevation biases over stable terrain that is assumed to have not undergone surface changes between the dates of the two DEMs. Unstable terrain should be defined by the analyst. It would normally include the landslide area or water bodies that is masked out during the alignment process and the quality assessment. Additional methods such as deramping, which removes non-linear co-registration biases such as tilts and rotations, are also supported. For the error assessment, *xDEM* implements the normalized median absolute deviation (NMAD), among other measurements, to estimate the bias to a reference DEM. As a next step, we implement this metric in relation to LULC, slope and aspect categories to identify areas where the elevation values from the generated DEMs present larger errors.

The *volume* module computes the DoD based on pre- and post-event Sentinel-1 co-registered DEMs. The DoD allows the computation of the landslide volume, which is then compared to a reference volume estimation. Ideally, a reference DoD is available to compare the spatial distribution of the elevation difference errors.

The workflow relies on several software and Python packages, all of which have their own dependencies on specific software versions and operating systems. To improve the usability of the workflow, we distribute the "SliDEM" package along with a Dockerfile based on an Ubuntu-based Docker image for SNAP-8, distributed by Mundialis (Tawalika and Neteler, 2022). With this Dockerfile, the analyst can build a container with a mounted volume to read and write on its local disk. Moreover, we implemented two different conda environments that allow to work with different versions of the same software for different tools. The final package will be released under an open-source license in a public GitHub repository.

The proposed workflow brings several advantages, for example, 1) cross-platform usage, when Docker is available; 2) easy update implementation, because it would only require the re-build of the Docker image; 3) its implementation as a Python package, which easily interoperates with the available Python APIs for Sentinel-1 processing; 4) significantly less time-consuming manual query tasks before Sentinel-1 scene download; and 5) the possibility of generating DEMs in an iterative and structured manner, which speeds up the analysis process, allows the processing of several scenes, and allows the analyst to focus on the results rather than on technical glitches.

However, this implementation also has limitations, such as 1) dependence on other open-source projects for major updates, for example, from SNAP-8 to SNAP-9 or the latest SNAPHU versions; 2) the lack of a GUI, which for some analysts can be cumbersome because they are not familiar with CLI or working within a Docker container. Further improvements include launching the Docker container with a Jupyter notebook as an entry point, which would allow for more user interaction.

4. CASE STUDIES

4.1 Study areas

Landslides from distinct landslide-prone regions in Austria and Norway serve as examples for method development and workflow testing and evaluation in terms of reliability, performance, reproducibility, and transferability. The study areas exhibit different environmental characteristics (e.g., climatic, LULC, and lithological settings) and landslide types and sizes, which makes them well-suited for testing and demonstrating the applicability and transferability of our research. To demonstrate the current workflow, we present preliminary results for two major landslide events (Figure 3).

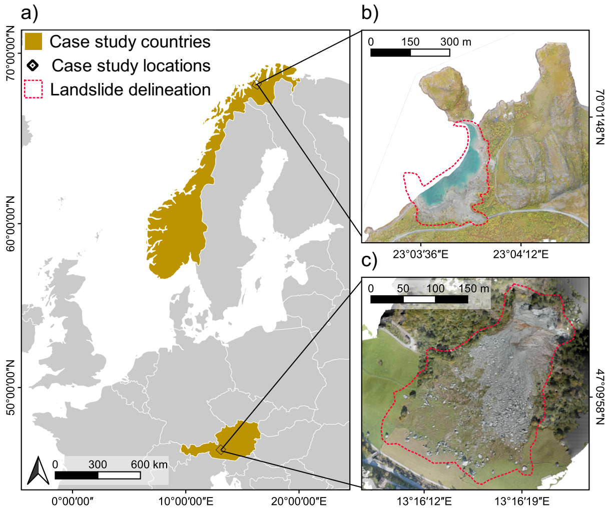

Figure 3: Study areas. a) Location of the landslides in Norway and Austria. b) Landslide in Kråknes, Alta, Norway, shown on a post-event RGB orthophoto generated from UAV images taken on 11.09.2021. c) Rockfall in Hüttschlag, Grossarl, Austria, shown on a post-event RGB orthophoto generated from UAV images taken on 15.10.2021.

In Austria, we focus on the rockfall in Hüttschlag, Grossarl Valley, State of Salzburg (ORF, 2019). Between spring and autumn 2019, recurring rockfall activity occurred with rockfall boulders up to the size of single-family houses. There is still a high risk of further rockfall activity, as indicated by cracks above the scar. This rockfall is located in the High Tauern Mountain range in the Central Eastern Alps, in a narrow valley with steep topography.

In Norway, we test our workflow for a major event in the northern part of the country, i.e. the quick clay landslide at Kråknes near Alta (NRK, 2020). The quick clay landslide occurred on June 3, 2020. It destroyed several houses but did not lead to fatalities. Another retrogressive failure happened two days later and destroyed the old E6 road (NVE, 2020). The quick clay landslide occurred in a coastal area, where most of the debris went underwater. Elevations do not exceed 200 m in this area, and the topography is less steep than that in the Austrian study area.

4.2 DEM generation and volume estimation results

Preliminary results for the two selected landslide events are presented and discussed in this section. Sentinel-1 image pairs from before and after the landslide events were downloaded and used for further processing. For both case studies, we worked with B_{perp} thresholds between 120 and 200 and B_{temp} thresholds between 6 and 60 days. The selected image pairs are shown in Table 1. They were all in VV polarisation mode and had a modelled coherency above 0.8, which indicates a high correlation between the SAR image pairs.

The DEM generation module was run for the four image pairs selected using the Copernicus DEM with 30 m spatial resolution for back-geocoding and terrain correction. The resulting DEMs were resampled to 30 m spatial resolution. They were vertically aligned using a deramping approach, which only corrects vertical shifts based on the stable terrain of the reference pre-event DEMs. For the Austrian study area this was a 1 m resolution DTM based on LiDAR campaigns between 2013 and 2018, and for Norway a 0.5 m resolution LiDAR digital terrain model (DTM) from 29.07.2018.

AOI	Dates	Path (Pass)	B_{temp}	B_{perp}	MC
			days	m	-
Hüttschlag, Grossarl, Austria	30.08. & 05.09.2018	44 (Asc.)	6	139	0.87
	12.07. & 30.07.2020	95 (Desc.)	18	128	0.88
Kråknes, Alta, Norway	12.06. & 18.06.2019	95 (Desc.)	6	152	0.88
	05.06. & 29.07.2020	87 (Asc.)	54	192	0.84

Table 1: Sentinel-1 image pairs for DEM generation per Area of Interest (AOI). B_{temp} stands for temporal baseline, B_{perp} for perpendicular baseline, MC for modelled coherency, $Asc.$ for ascending pass and $Desc.$ for descending pass.

Figures 4a and 4b show the pre- and post-event DEMs generated from Sentinel-1 imagery for Hüttschlag, Grossarl, Austria, where the rockfall area is delineated by a dashed red line. Figures 4d and 4e show the reference pre- and post-event DEMs for comparison. We can observe a strong overestimation of the elevation values, even after vertical co-registration. Table 2 lists the estimated errors between the generated and the reference DEMs. The Hüttschlag area presents a deviation between 211 m and 170 m for the pre- and post-event Sentinel-1 DEMs, respectively. Figure 4c shows the DoD for the Sentinel-1-based DEMs, where the results contradict the actual volume loss and gain areas, as compared to Figure 4f, which shows the DoD between the reference DEMs.

AOI	Dates	NMAD
		m
Hüttschlag, Grossarl, Austria	30.08. & 05.09.2018	211.4
	12.07. & 30.07.2020	173.6
Kråknes, Alta, Norway	12.06. & 18.06.2019	11.9
	05.06. & 29.07.2020	38.4

Table 2: Quality assessment of the generated DEMs. AOI: Area of interest, NMAD: normalized median absolute deviation.

Table 3 lists the volume calculations for the source and deposition areas. These figures were calculated for the reference DoDs and for the Sentinel-1 based DoDs per study area. Table 3 also shows the volume reported in official reports or newspapers. The estimated volume for the Sentinel-1-based DoD resulted in 3.8 million m^3 of deposited material, a volume approximately eighty times higher than the reference volume. In contrast, the material lost from the source area seems to agree better with the calculated reference source volume, with a surplus of 10 thousand m^3.

The results for the Kråknes landslide are shown in Figure 5. Figures 5a and 5b show the pre- and post-event DEMs generated from the Sentinel-1 imagery. Figures 5d and 5e show the reference pre- and post-event DEMs for comparison. In this case, we can observe a better match between elevation values, where the post-event DEM shows a slight overestimation of approximately 40 m, whereas the pre-event DEM shows a deviation of 12 m (Table 2). The pre-event DEM was further processed to remove sinkholes. Figure 5c shows the DoD for the Sentinel-1-based DEMs, where an elevation gain can be observed in the lower left area of the landslide. In comparison with Figure 5f, which shows the DoD between the reference DEMs, we can observe negative elevation differences for both, whereas the Sentinel-1-based DoD shows an overestimation. In any case, this results in a much better agreement than in the Austrian case for the elevation differences.

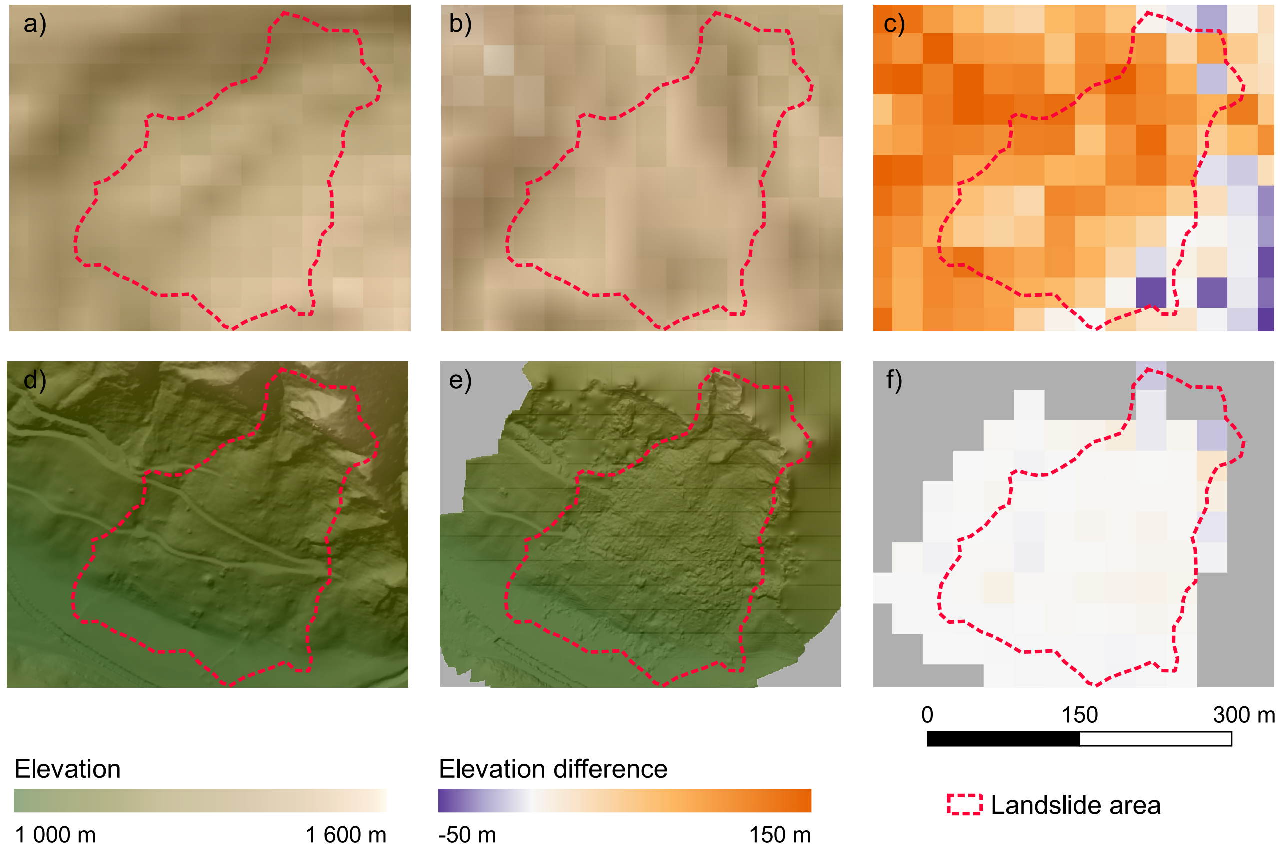

Figure 4: Initial result for Hüttschlag, Grossarl, Austria. a) Pre-event DEM based on Sentinel-1 from 30.08. & 05.09.2018. b) Post-event DEM based on Sentinel-1 from 12.07. & 30.07.2020. c) DEM of Difference (DoD) between post- and pre-event DEMs based on Sentinel-1. d) Pre-event DTM based on LiDAR campaigns between 2013 and 2018 (© SAGIS). e) Post-event DTM based on UAV acquisition from 15.10.2021. f) DoD between the post-event UAV DTM and the pre-event LiDAR DEM.

Given the gentler slopes for the Norwegian study sites, the quality of the generated DEMs from Sentinel-1 is better, although the proximity to water introduced negative elevation values in inland areas, requiring further post-processing of the result. Regarding the volume estimation (Table 3), we observe that the calculated deposition volume is within a similar range, with an underestimation for the Sentinel-1 based DEM, while the source volume is greatly overestimated in comparison to the reference volume computed.

AOI		Reference volume	S-1-based volume
		m^3	m^3
Hüttschlag, Grossarl, Austria	Literature Deposition Source	22,500.0 43,555.2 55,640.8	- 3 868,217.8 65,182.1
Kråknes, Alta, Norway	Literature Deposition Source	600,000.0 599,721.4 1,681.7	- 568,438.4 1 653,657.7

Table 3: Volume estimation. AOI: Area of interest, S-1: Sentinel-1.

These results are strongly influenced by 1) the steep topography and vegetation, 2) atmospheric conditions, e.g., presence of water vapour, which can cause temporal baseline decorrelation, and 3) stochastic errors introduced during data processing, e.g., during the phase unwrapping process (Colesanti and Wasowski, 2006). Even if the quality of the Sentinel-1-based DEMs varies among the study areas, the preliminary results are promising. However, there is a need for improvement and thorough analysis of the causes of elevation errors. Further analysis of SAR related factors, such as flight pass, suitable perpendicular and temporal baselines, topographic factors, e.g., slope and aspect, as well as environmental factors, e.g., LULC, needs to be performed to identify key limitations and to enhance the quality of the DEMs. The possibility of iteratively generating DEMs within the “SliDEM” workflow allows for systematic evaluation of these factors. Once a good DEM quality is achieved, landslide volume estimations will also become more accurate and reliable.

5. CONCLUSION

The workflow implemented within the “SliDEM” Python package represents an important contribution to the field of natural hazard research by developing an open-source, low-cost, transferable, and semi-automated method for DEM generation and landslide volume estimation. We used the “SliDEM” package on the two selected case study areas to test the workflow implementation, identify key input parameters, detect bugs and common errors, improve the performance, and assess its usability. This iterative process allows for continuous improvement of the workflow.

From a practical perspective, disaster risk management can benefit from efficient methods that deliver added-value information. From a technical point of view, it tackles scientific questions regarding the validity of EO-based methods and the quality of the results

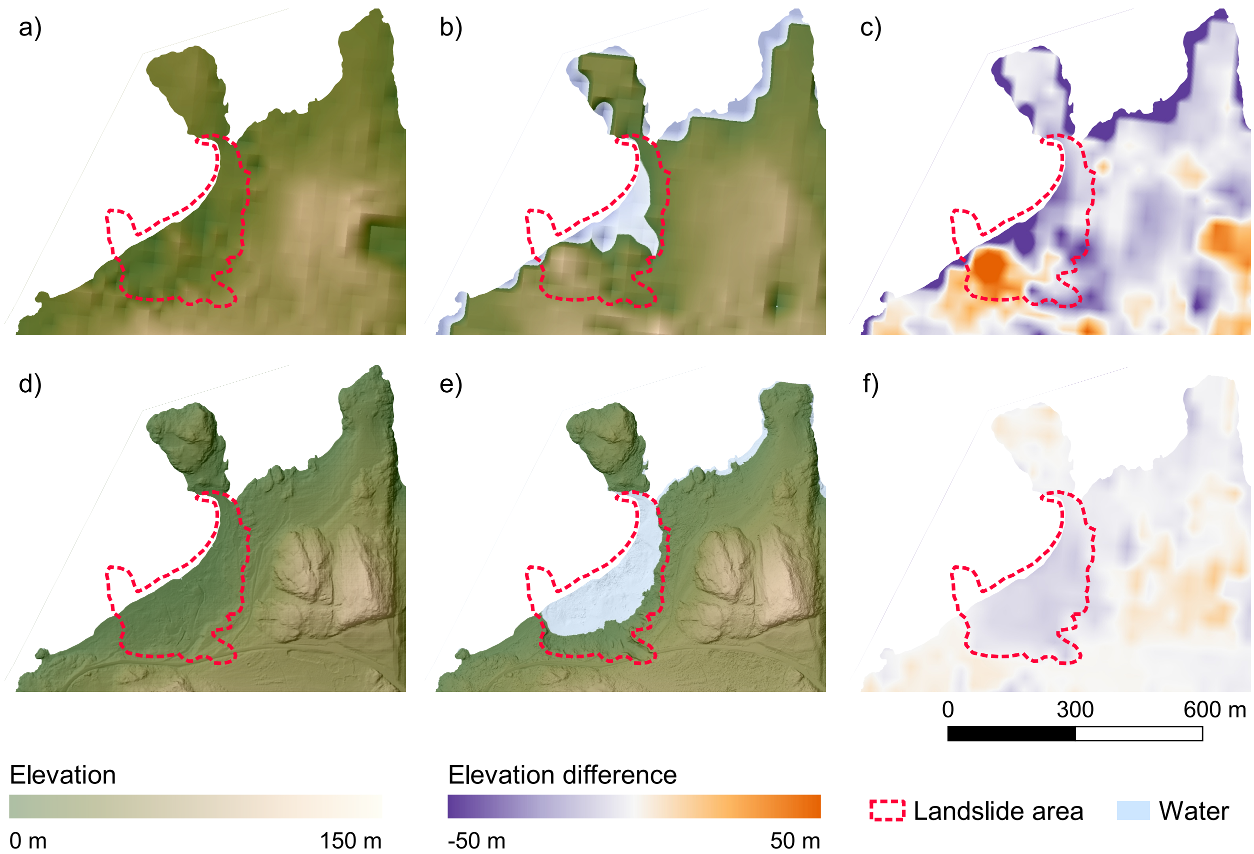

Figure 5: Initial result for Kråknes, Alta, Norway. a) Pre-event DEM based on Sentinel-1 from 12.06. & 18.06.2019. b) Post-event DEM based on Sentinel-1 from 05.06. & 29.07.2020. c) DEM of Difference (DoD) between post- and pre-event DEMs based on Sentinel-1. d) Pre-event LiDAR DTM from 29.07.2018 (© Kartverket). e) Post-event DTM based on UAV acquisition for 11.09.2021. f) DoD between the post-event UAV DTM and the pre-event LiDAR DTM.

related to the assessment of the geomorphological characteristics of landslides.

ACKNOWLEDGEMENTS

This work is supported by the Austrian Research Promotion Agency (FFG) through the project SliDEM (Assessing the suitability of DEMs derived from Sentinel-1 for landslide volume estimation; contract no. 885370).

REFERENCES

Alaska Satellite Facility DAAC, 2019. How to Create a DEM using Sentinel-1 Data. Alaska Satellite Facility DAAC. Data Recipes (24 November, 2020).

Alaska Satellite Facility Discovery Team, 2022. asf-search: Python wrapper for ASF's SearchAPI, Version 3.2.2. Alaska Satellite Facility. pypi.org/project/asf-search (20 May 2022).

Argentin, A. L., Robl, J., Prasicek, G., Hergarten, S., Hölbling, D., Abad, L. and Dabiri, Z., 2021. Controls on the formation and size of potential landslide dams and dammed lakes in the Austrian Alps. Natural Hazards and Earth System Sciences 21(5), pp. 1615–1637. doi.org/10.5194/NHESS-21-1615-2021.

Atefi, M. R. and Miura, H., 2021. Volumetric Analysis of the Landslide in Abe Barek, Afghanistan Based on Nonlinear Mapping of Stereo Satellite Imagery-Derived DEMs. Remote Sensing. doi.org/10.3390/rs13030446.

Bamler, R. and Hartl, P., 1998. Synthetic aperture radar interferometry. Inverse Problems 14(4), pp. R1–R54. doi.org/10.1088/0266-5611/14/4/001.

Bernard, T. G., Lague, D. and Steer, P., 2021. Beyond 2D landslide inventories and their rollover: synoptic 3D inventories and volume from repeat lidar data. Earth Surface Dynamics 9(4), pp. 1013–1044. doi.org/10.5194/esurf-9-1013-2021.

Braun, A., 2020. DEM generation with Sentinel-1 Workflow and challenges. Technical report, SkyWatch Space Applications Inc.

Braun, A., 2021. Retrieval of digital elevation models from Sentinel-1 radar data – open applications, techniques, and limitations. Open Geosciences 13(1), pp. 532–569. doi.org/10.1515/geo-2020-0246.

Brito, F., 2022. snapista: SNAP GPT thin layer for Python. GitHub. github.com/snap-contrib/snapista (24 May 2022).

Brotoisworo, P., 2021. S-1 TOPS SPLIT Analyzer (STSA). GitHub. github.com/pbrotoisworo/s1-tops-split-analyzer (20 May, 2022).

Bürgmann, R., Rosen, P. A. and Fielding, E. J., 2000. Synthetic Aperture Radar Interferometry to Measure Earth's Surface Topography and Its Deformation. Annual Review of Earth and Planetary Sciences 28(1), pp. 169–209. doi.org/10.1146/annurev.earth.28.1.169.

Chang, K.-j., Tseng, C.-W., Tseng, C.-m., Liao, T.-c. and Yang, C.-j., 2020. Application of Unmanned Aerial Vehicle (UAV)-

Acquired Topography for Quantifying Typhoon-Driven Landslide Volume and Its Potential Topographic Impact on Rivers in Mountainous Catchments. Applied Sciences 10(17), pp. 6102. doi.org/10.3390/app10176102.

Chen, C. and Zebker, H., 2002. Phase unwrapping for large SAR interferograms: statistical segmentation and generalized network models. IEEE Transactions on Geoscience and Remote Sensing 40(8), pp. 1709–1719. doi.org/10.1109/TGRS.2002.802453.

Colesanti, C. and Wasowski, J., 2006. Investigating landslides with space-borne Synthetic Aperture Radar (SAR) interferometry. Engineering Geology 88(3-4), pp. 173–199. doi.org/10.1016/j.enggeo.2006.09.013.

Crosetto, M., 2002. Calibration and validation of SAR interferometry for DEM generation. ISPRS Journal of Photogrammetry and Remote Sensing 57(3), pp. 213–227. doi.org/10.1016/S0924-2716(02)00107-7.

Dabiri, Z., Hölbling, D., Abad, L., Helgason, J. K., Sæmundsson, Þ. and Tiede, D., 2020. Assessment of Landslide-Induced Geomorphological Changes in Hítardalur Valley, Iceland, Using Sentinel-1 and Sentinel-2 Data. Applied Sciences 10(17), pp. 5848. doi.org/10.3390/app10175848.

Dehecq, A., Mannerfelt, E., Hugonnet, R., Knuth, F. and Tedstone, A., 2021. xDEM: Set of tools to manipulate Digital Elevation Models (DEMs), Version 0.0.2. Zenodo. doi.org/10.5281/zenodo.4809698.

European Space Agency, 2022. S1TBX - ESA Sentinel-1 Toolbox, Version 8.0.9. European Space Agency. step.esa.int. (24 May 2022).

European Space Agency and Brockmann Consult, 2022. snappy: SNAP-Python module of ESA's Sentinel Applcation Platform (SNAP). European Space Agency. github.com/senbox-org/snap-engine (24 May 2022).

NRK, 2020. Åtte bygninger feid på sjøen i jordskred i Alta (Eight buildings swept at sea in landslides in Alta). NRK Troms og Finnmark. nrk.no/tromsogfinnmark/stort-jordras-har-gatt-i-alta-1.15039394 (26 November, 2020).

Nuth, C. and Kääb, A., 2011. Co-registration and bias corrections of satellite elevation data sets for quantifying glacier thickness change. The Cryosphere 5, pp. 271–290. doi.org/10.5194/tc-5-271-2011.

NVE, 2020. Kvikkleireskredet i Alta: NVE undersøker grunnforholdene (The quick clay landslide in Alta: NVE investigates the ground conditions). Norwegian Water Resources and Energy Directorate (NVE). nve.no/nytt-fra-nve/nyheter-skred-og-vassdrag/kvikkleireskredet-i-alta-nve-undersoker-grunnforholdene/ (24 November, 2020).

ORF, 2019. Hüttschlag: Lage nach Felssturz angespannt (Hüttschlag: Situation tense after rock fall). ORF. salzburg.orf.at/stories/3020136 (26 November 2020).

Paulin, G. L., Mickelson, K. A., Contreras, T. A., Gallin, W., Jacobacci, K. E. and Bursik, M., 2022. Assessing landslide volume using two generic models: application to landslides in Whatcom County, Washington, USA. Landslides 19(4), pp. 901–912. doi.org/10.1007/s10346-021-01825-z.

Robson, B. A., Hölbling, D., Nielsen, P. R. and Koller, M., 2022. Estimating the volume of the 1978 Rissa quick clay landslide in Central Norway using historical aerial imagery. Open Geosciences 14(1), pp. 252–263. doi.org/10.1515/geo-2020-0331.

Santangelo, M., Zhang, L., Rupnik, E., Deseilligny, M. P. and Cardinali, M., 2022. Landslide evolution pattern revealed by multi-temporal DSMs obtained from historical aerial images. Int. Arch. Photogramm. Remote Sens. Spatial Inf. Sci. XLIII-B2-2022, pp. 1085–1092. doi.org/10.5194/isprs-archives-XLIII-B2-2022-1085-2022.

Tawalika, C. and Neteler, M., 2022. ESA SNAP 8 docker image. DockerHub. hub.docker.com/r/mundialis/esa-snap (18 March 2022).

Tsutsui, K., Rokugawa, S., Nakagawa, H., Miyazaki, S., Cheng, C.-T., Shiraishi, T. and Yang, S.-D., 2007. Detection and Volume Estimation of Large-Scale Landslides Based on Elevation-Change Analysis Using DEMs Extracted From High-Resolution Satellite Stereo Imagery. IEEE Transactions on Geoscience and Remote Sensing 45(6), pp. 1681–1696. doi.org/10.1109/TGRS.2007.895209.

Turner, D., Lucieer, A. and de Jong, S. M., 2015. Time series analysis of landslide dynamics using an Unmanned Aerial Vehicle (UAV). Remote Sensing 7(2), pp. 1736–1757. doi.org/10.3390/rs70201736.

Ventura, G., Vilardo, G., Terranova, C. and Sessa, E. B., 2011. Tracking and evolution of complex active landslides by multi-temporal airborne LiDAR data: The Montaguto landslide (Southern Italy). Remote Sensing of Environment 115(12), pp. 3237–3248. doi.org/10.1016/j.rse.2011.07.007.

APPENDIX

The repository of the "SliDEM" Python package (work in progress) can be accessed here: `https://github.com/SliDEM-project/SliDEM-python`